The influence of the procedure of iron doping of CVD-ZnSe using high-temperature diffusion on the composition and spatial distribution of impurity-defect centers

© V.P. Kalinushkin[1], O.V. Uvarov[1], A.A. Gladilin[1], S.A. Mironov[1,¶], M.V. Poplavskiy[1], P.D. Pupyrev[2], E.M. Gavrischuk[3], D.V. Savin[3], N.A. Timofeeva[3]

[1] Prokhorov Institute of General Physics, Russian Academy of Sciences, 119991 Moscow, Russia
[2] Kotelnikov Institute of Radio Engineering and Electronics, Russian Academy of Sciences, 111250 Moscow, Russia
[3] Devyatykh Institute of Chemistry of High-Purity Substances, Russian Academy of Sciences, 603951 Nizhny Novgorod, Russia

¶ E-mail: sa.mironov@kapella.gpi.ru

Received May 7, 2024
Revised November 28, 2024
Accepted December 5, 2024

The spatial distribution of impurity-defect centers in CVD-ZnSe crystals formed after the procedure of doping these crystals with iron using high-temperature doping is investi- gated.The experiments were carried out using the method of two- photon confocal microscopy, which allows recording luminescence in the range of $0.44-0.73\,\mu$m with a spatial resolution of several μm. It is shown that as a result of this procedure, the crystal becomes significantly inhomogeneous not only in the doping zone. Regions hundreds of microns in size are formed in it adjacent to all its surfaces with a composition of intrinsic point defects and their complexes different from the main volume. It is found that the sizes of these regions depend on the doping time. Assumptions are made about the nature of complexes of intrinsic defects with residual impurities formed during doping and the mechanism of formation of the above regions.

Keywords: ZnSe : Fe; two-photon confocal microscopy, impurity-defect composition, diffusion.

DOI: 10.61011/SC.2024.12.60387.6864

1. Introduction

Semiconductor doping by means of high-temperature diffusion (HTD) is an essential part of many technological processes. However, during these processes, significant changes in the characteristics of semiconductor materials can occur, not only in the doping range, but also in the crystal areas where the doping component is virtually non-existent. Perhaps, vaporization of one or another component of the semiconductor during HTD, formation or rearrangement of various structure defects and intrinsic point defects etc. For example, during HTD in CVD-ZnSe, the process of recrystallization of grains [1,2] occurs. Many works have been devoted to these processes. Their main focus was on the changes occurring either in the doping range or in the whole volume of crystals. At the same time, the authors of this article are not aware of any works in which the spatial distribution of these or those characteristics outside the doping range was studied in detail. However, it is possible that semiconductor crystals can become significantly heterogeneous in their properties not only in the doping range. The purpose of this work is to investigate the possible effect of the HTD procedure on the homogeneity of crystals that have undergone this procedure. At the same time, the primary focus will be on the study of the parts of the samples that are outside the doping range. For such experiments it is necessary to use methods with high spatial resolution and allowing the study of large volumes of crystals. In this paper we attempt to investigate the effect of iron doping of CVD-ZnSe crystals by means of HTD on the spatial distribution of luminescence characteristics of the whole sample subjected to this procedure. The use of luminescence to study the characteristics of crystals is due to the fact that this technique is highly sensitive to the presence of impurity-defect centers (IDC) in crystals. In addition, the authors have a technique for recording the luminescence characteristics of ZnSe crystals with a spatial resolution of several microns, which allows us to study areas in the crystal volume at distances up to several millimeters from their surface (two-photon confocal microscopy — TPEF). This technique combines good spatial resolution, the ability to study relatively large volumes of crystals, and high rapidity of experiments. Thus, the luminescence characteristics in the $0.44-0.72\,\mu$m range of an $1\times1\times2\,\mu$m portion of a crystal can be determined in 10 min with a spatial resolution of a few microns [3,4].

The choice of the investigated material is connected with the fact that in the case of two-component semiconductors the influence of high-temperature heat treatments on their characteristics should be greater than in monoatomic

crystals due to the difference in the evaporation rate of different components. Also, CVD-ZnSe-Fe crystals doped with HTD are widely used to create mid-IR lasers [5–9]. The works on increasing the efficiency of the systems created on the basis of these lasers require the study of the composition and spatial distribution of IDC in these crystals.

2. Experiment description

High-purity polycrystalline CVD-ZnSe was used as the starting material in all experiments. In the study, a series of iron-doped polycrystals were investigated at a temperature of 1000°C in an Ar atmosphere and a pressure of 1 atmosphere. The annealing times were 8, 12, 20, 40, and 90 h (samples 1–5 respectively). Iron-doped crystals doped in zinc vapor atmosphere at 1 atmosphere 1000°C temperature for 20 h (sample 6) and undoped ZnSe samples annealed in zinc and argon atmospheres (1000°C, pressure 1 atmosphere, time 72 h, samples 7, 8) were also studied. A detailed description of the high-temperature diffusion doping technique is given in [2].

The impurity composition of the samples before and after doping was analyzed by inductively coupled plasma atomic emission spectrometry (AES–ICP). The results are given in the table. The table shows that there was no significant contamination by side impurities during doping.

The studied samples had the shape of parallelepipeds with the size of $10 \times 15 \times 2.7$ mm. The doping was carried out from one surface of size 10×15 mm. This surface will be further referred to as the „doping surface". The surfaces perpendicular to it will be designated as „surfaces of chipping", the opposite doping surface — as „free" surface. The crystal edges between the doping surface and the chipping surface will be called doping edges, between the chipping surfaces — chipping edges, between the free surface and the chipping surfaces — free edges.

The luminescence characteristics and their spatial distribution were investigated using TPEF. TPEF studies were carried out using a Carl Zeiss LSM 710 NLO confocal microscope. The main attention was paid to the determination of the spatial distribution of IDC luminescence in the spectral range 480–725 nm. A detailed description of the technique is provided in [3,4].

The concentration profile of iron was determined according to the method developed in [11].

The results of the study of the doping range and the adjacent part of 1–5 crystals are given in [10]. However, in this work, a small part of the sample volume was investigated. The depth of the doping range in these samples did not exceed 500 μm. In [10] this range of the crystal and the adjacent region with a depth of also $\sim 500\,\mu$m were investigated. Thus, the total depth of the crystal area investigated in [10] did not exceed 1 mm. In addition, a part of this region with a width of 2 mm and at a distance from the surface „of the chipping" at 200–400 μm was investigated. Thus, in a sample of size $10 \times 15 \times 2.7$ mm, a parallelepiped of size $2 \times 1 \times 0.2$ mm was investigated. In this study, the entire volume of these crystals will be investigated.

Impurity composition, wt.%

Impurity	Initial CVD-ZnSe	Fe^{2+}:ZnSe (Ar, 1000°C, 90 h)
Al	$3 \cdot 10^{-5}$	$3 \cdot 10^{-5}$
Ca	$< 2 \cdot 10^{-5}$	$4 \cdot 10^{-5}$
Cr	$< 3 \cdot 10^{-6}$	$7 \cdot 10^{-5}$
Cu	$4 \cdot 10^{-4}$	$3 \cdot 10^{-4}$
Fe	$< 2 \cdot 10^{-5}$	$3 \cdot 10^{-3}$
K	$< 4 \cdot 10^{-4}$	$< 4 \cdot 10^{-4}$
Mg	$3 \cdot 10^{-4}$	$7 \cdot 10^{-6}$
Mn	$< 5 \cdot 10^{-6}$	$< 5 \cdot 10^{-6}$
Mo	$< 1 \cdot 10^{-4}$	$< 1 \cdot 10^{-4}$
Na	$4 \cdot 10^{-5}$	$4 \cdot 10^{-5}$
Ni	$< 4 \cdot 10^{-5}$	$< 5 \cdot 10^{-5}$
Si	$< 1 \cdot 10^{-4}$	$< 1 \cdot 10^{-4}$

3. Results

Figure 1 shows flat luminescence maps of the sample doped with iron in argon atmosphere for 20 h (sample 3) taken at a wavelength of 541 nm at the distances from the surface of the „of the splinter" 40, 200 and 350 μm, respectively, and luminescence spectra in the 480–700 nm range of different regions of this crystal.

Figure 2 shows detailed flat luminescence maps of the luminescence areas *1, 3* of the same sample at wavelengths 541 and 628 nm. Also shown are the dependences of the luminescence intensity at wavelengths 541 and 628 nm on the distance from „of the free" facet and the „facets of the chipping" and doping, taken from the regions shown in the flat maps shown in Figure 2.

It can be seen that the areas on all sides of the crystal adjacent to its surfaces differ from the main volume of the crystal in their luminescence characteristics. The following areas of the crystal can be distinguished:

1 — the area of the crystal adjacent to the „doping" surface;

2 — the area of the crystal adjacent to the chipping „surface";

3 — the area of the crystal adjacent to „the free surface";

area *4* — the main volume of the crystal, which does not include the areas *1, 2* and *3*.

The area *1* (doping range) was investigated in [10]. It consists of an area with a high ($\sim 10^{19}-10^{18}$ cm^{-3}) concentration of iron ions, in which luminescence in the entire spectral range is suppressed — the so-called „dead" area. Its width in this crystal is $\sim 50\,\mu$m. It is adjoined by a broad (100 μm in this crystal) band parallel to the doping surface with high luminescence intensity in the range of 520–541 nm (Figures 1, 2). The concentration of iron ions

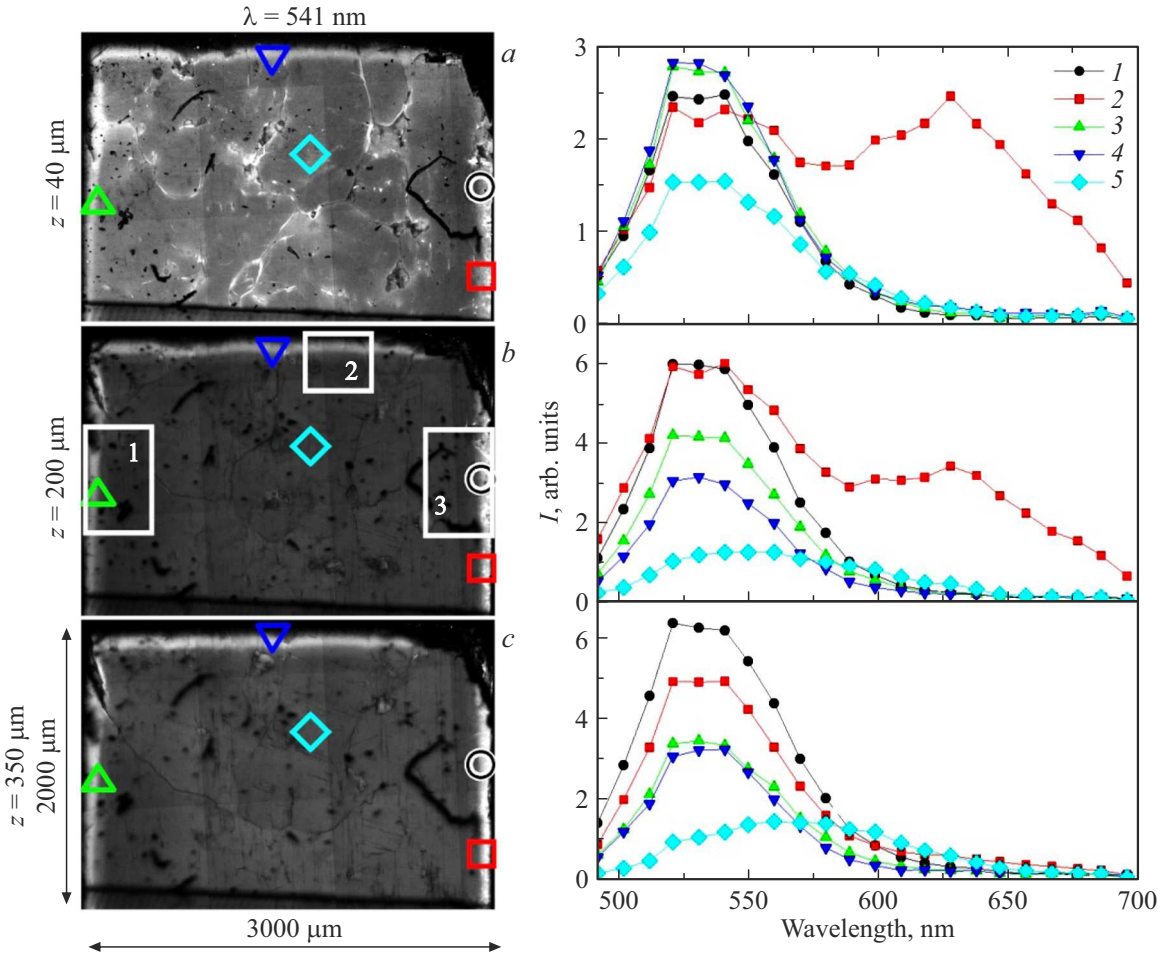

Figure 1. Flat luminescence maps at 541 nm and spectra at the indicated points of the sample 3 at distances of 40 (a), 200 (b), and 350 μm (c) from the „surface of the chip“.

in it falls to 10^{17} cm^{-3} and becomes below the detection limit of the technique used. The luminescence spectrum of this part of the crystal is dominated by a broad band with a maximum of 520–541 nm (line 541, Figure 1). The intensity of the line 541 increases with increasing distance from the doping edge. It reaches its maximum at the distance $\sim 100\,\mu$m (Figure 2). Then its intensity begins to decrease, resulting in the formation of the enhanced luminescence intensity area (ELIA) of this line in the form of a band parallel to the doping surface. At the distance $\sim 200\,\mu$m from the doping face, the intensity of the line 541 reaches a plateau (Figure 2). The ELIA line looks like a fairly regular line parallel to the surface, which is slightly curved in the case of crossing it by the grain boundary (Figure 1, 2). This type of ELIA indicates that the ELIA line was formed as a result of diffusion of some point defects deep into the crystal. The shape of the line spectrum in the *1* area independent of the distance from the chipping surface (Figure 1).

The *2* area is close to the luminescent characteristics of the *1* area. Both the dead area and the ELIA area are also registered in it. The parameters of these regions are similar to the characteristics of the same regions in the area *1* (Figures 1, 2).

The area *4* can be conditionally divided into at least two areas. The luminescence of the part of the area *4* located at a distance less than or $\sim 50\,\mu$m from the „surface of the chip“ has a spectral composition close to the spectra in ELIA — line 541 nm (Figure 1, a). The situation changes when examining the regions of the area *4* located at a distance $> 50\,\mu$m from the surface „of the chipping“. As can be seen in Figure 1, b, in the luminescence spectrum of the area region *4* located at a distance of 200 μm from the chip surface, a shift of the luminescence intensity maximum of the line 541 to the long-wavelength area is observed. It shifts to 560 nm. Further shifting the region of investigation into the depth of the sample shifts the line 541 to a line with a luminescence intensity maximum near 570–580 (line 570) in the entire volume. As a result, as can be seen from Figure 1, c, the spectrum of the part of the area *4* located at a distance of 350 μm from the chip surface is homogeneous. It is dominated by the line 570.

The results of the area *1* and the part of the area *4* located at distances $> 200\,\mu$m from the chip surface are similar to

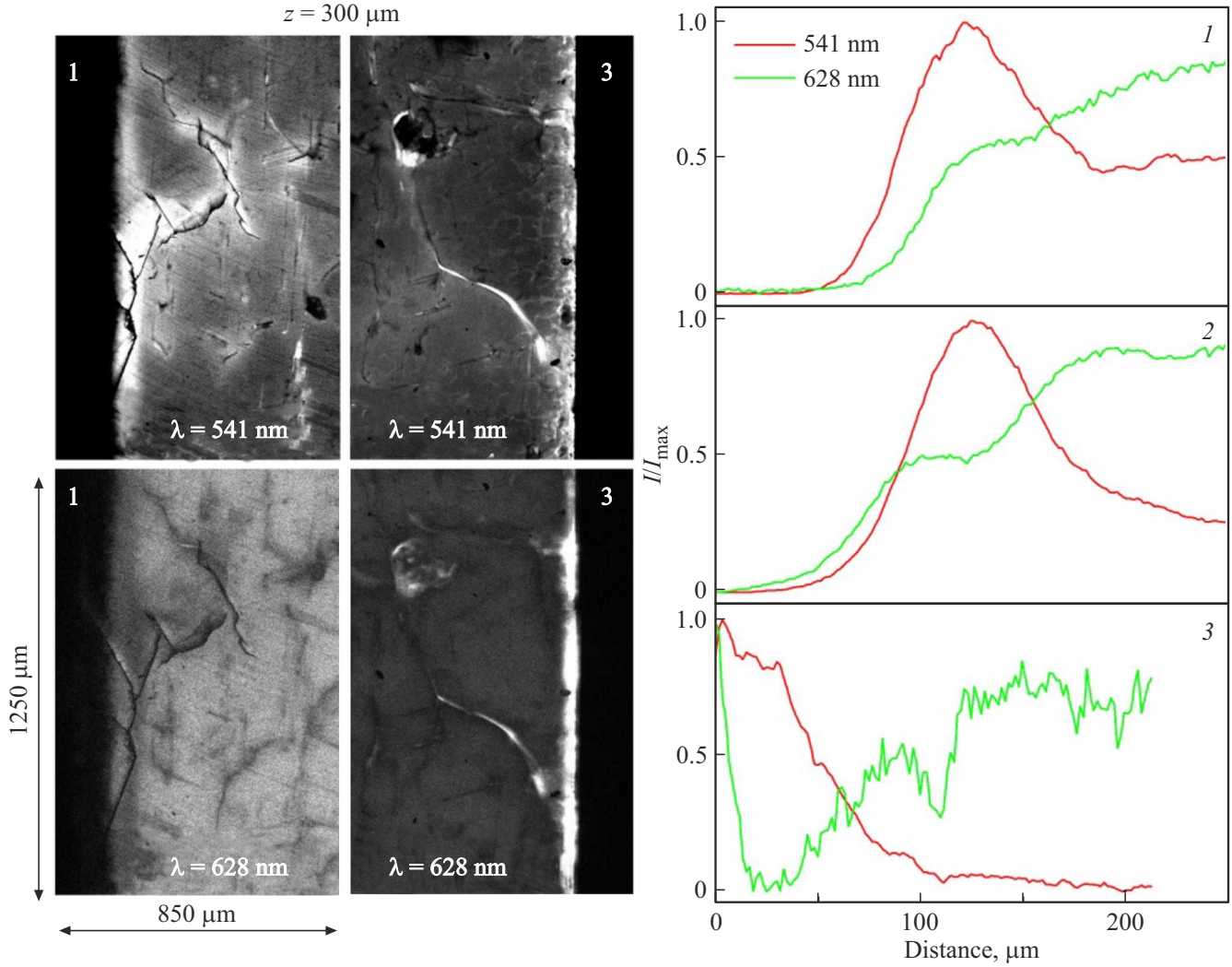

Figure 2. A flat map of the luminescence of a sample 3 at 628 nm and a distance of 300 μm from the surface of the "chipped". The diagrams show the distribution of luminescence intensity at these wavelengths as a function of the distance from the „doping" facet (graph *1*), the „facet" (graph *2*), and the „free" facet (graph *3*).

the results obtained in [10]. In the area *1*, a dead area and an ELIA area are also recorded. The luminescence spectra in the ELIA area and part of the above area *4* observed in this study are also similar to those recorded in [10]. However, in [10], a small fraction of crystals located at a distance of $> 200\,\mu$m from its surface were investigated. Accordingly, there is no information in [10] that the luminescence characteristics of the part of the area *4* adjacent to the surface of the „of the splinter" are similar to those of the ELIA area and differ significantly from those of the rest of the area *4*.

The area *3* has also not been investigated in [10]. As can be seen from Figure 1, its spectrum consists of a line close to the line 541 and a broad line with a maximum near 628 nm (line 628). In this part of the crystal there is no „dead" area in which luminescence in the range under study is suppressed. The intensities of almost all lines are maximal at the free edge of the crystal. The intensities of the lines 541 and 628 are different in different regions of the area *3*. The intensity of the line 541 is more uniform in this area while the intensities of the line 628 vary significantly in different regions of the area *3* (Figures 1, 2). This area does not look monolithic-type in contrast to ELIA; it consists of areas of different sizes with different spectra and luminescence intensities. Its boundary with the area *4* is inhomogeneous. The luminescence intensities of all lines decrease with distance from the free edge of the chip (Figure 2). The luminescence intensity of the line 628 decreases most rapidly (Figure 2). The luminescence spectrum of the area *3* does not change at different distances from the chipping surface. However, the spatial distribution of regions with different luminescence characteristics in the area *3* at different distances from the chipping surface is different.

These results were typical for all series of samples doped with iron in argon atmosphere studied in this paper. Only

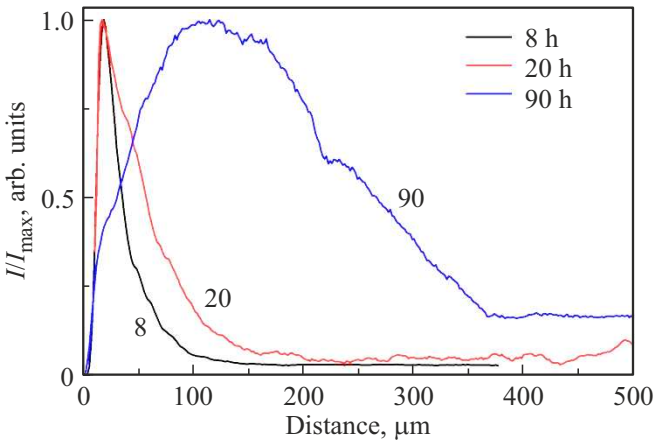

Figure 3. The normalized distribution of luminescence intensity at a wavelength of 541 nm from the distance from the doping surface of samples 1, 2 and 5 (doping time 8, 20 and 90 h, respectively).

the distance from the doping, „chipping" and „of free" surfaces occupied by the areas *1, 2, 3* varied. These changes for the area *1* are described in detail in [10]. Increasing the doping time leads to an increase in the dead area width and the distance to the exciton and luminescence intensity maxima 541. The width of the ELIA line also increased. As a result, the area width *1* reached 500 μm during doping for 90 h. The changes of the area width *2* were similar to those mentioned above. Figure 3 shows the dependence of the luminescence intensity of the line 541 on the distance from the free edge for crystals doped for 8, 20, and 90 h (i.e., actual area widths *3*). It can be seen that the area width *3* also increased with increasing doping time. The luminescence spectra of the ELIA and areas *3* and *4* of the whole series of 1–5 samples were unchanged.

In Figure 4, *a, b* shows the flat luminescence maps taken at wavelengths 541 and 628 nm, and at a distance from the surface of approximately 100 μm, and luminescence spectra from different regions of ZnSe crystals annealed at 1000°C for 72 h in zinc and argon atmospheres at a pressure of 1 atmosphere (samples 7 and 8). The annealing conditions were approximated to the doping conditions of the samples investigated in this study. It was assumed that the luminescence characteristics of the near-surface area of the crystal annealed in argon would be close to those of the area *3*. However, it can be seen that in the crystal annealed in argon atmosphere, the area adjacent to the surface has a homogeneous, reduced compared to the volume of luminescence intensity in the entire spectral range. Its spectrum consists of a weakly intense IDC luminescence line with a maximum near 550 nm. The luminescence characteristics of this area differ qualitatively from those of *3* samples 1–5. At the same time, the area of the crystal 8 annealed in zinc, adjacent to the surface,

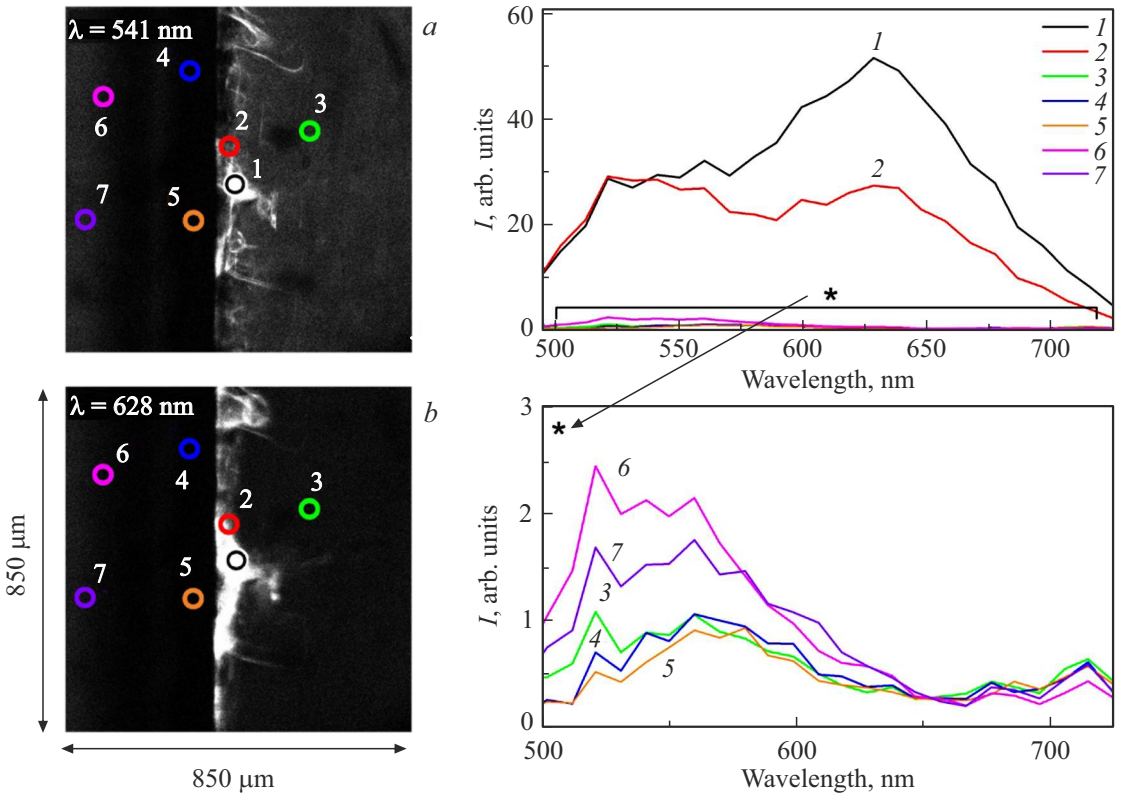

Figure 4. Flat luminescence maps at wavelengths 541 (*a*) and 560 nm (*b*) of samples *7* (annealed in zinc) and *8* (annealed in argon). The luminescence spectra in the above regions (regions *1–3* of sample *7*, points *4–6* — sample *8*) are shown in the plots.

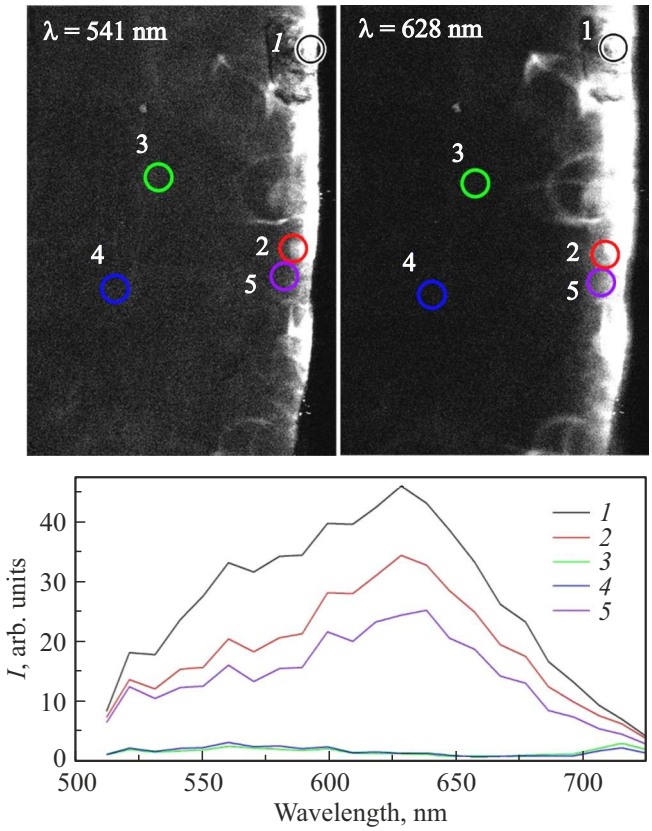

Figure 5. Flat luminescence maps at wavelengths 541 (*a*) and 640 nm (*b*) of the sample 6 and spectra in the above regions.

has luminescence characteristics close to the area *3* of the samples doped in argon. The spectrum of this part of the crystal 8 also consists of the luminescence of two IDC lines with maxima near 520−541 and 628 nm. Like the area *3*, this region consists of separate regions with different luminescence intensities.

Figure 5, *a, b* shows flat maps and luminescence spectra of different areas of an iron-doped ZnSe crystal in a zinc atmosphere at 1000°C for 20 h at a pressure of 1 atmosphere (sample 6) at wavelengths 541 and 638 nm. The portion of this sample adjacent to the „free“ surface is shown. It can be seen that this area of crystal 6 also has spectral characteristics similar to the luminescence characteristics of the area *3* of crystals 1−5. Its spectrum consists of a line with a maximum at 628 nm with high luminescence intensity, which merges with a line with maxima from 520 to 560 nm. This part of the crystal also consists of regions with different luminescence intensities.

4. Results and discussion

The results obtained can be explained based on the following models. During the deposition of iron film on ZnSe crystals, iron sputtering occurs not only on the doping surface but also on the chipping surface. The area *3* is covered by iron during sputtering, and iron does not fall on it or almost does not fall on it. As a result, during doping, dead areas and ELIA are formed in the areas *1* and *2* according to the mechanism proposed in [10]. These areas are formed on all surfaces of the „chip“. his explains the change in the luminescence spectral composition of the *4* area when the distance from the „surface of the“ chip is varied. The luminescence map taken at a distance of 50 μm from the „surface of the“ chip falls within the ELIA area. Accordingly, its spectrum is characteristic of this area of the crystal — line 541 nm. As the distance from the surface „of the chip“ of the carrier excitation area increases, the latter leaves the ELIA area adjacent to the surface of the chip, from which the excitation of carriers comes, and enters the area *4*. The luminescence spectra on flat maps taken at distances of 200 and 350 μm change accordingly. These spectra characterize the changes occurring in the composition of IDC in the main part of the crystal outside the doping area.

This assumption allows us to explain part of the results obtained. However, the fact that the area *3* of crystals doped with iron in an argon atmosphere is similar in its characteristics not to crystals annealed in argon, but annealed and doped in a zinc atmosphere, under this assumption is not explained. The following hypothesis is proposed to explain this fact. It is assumed that there is a process of formation of Zn_i atoms taking place simultaneously with the diffusion of iron ions, for example, as a result of the displacement of zinc ions from the node by iron ions. Part Zn_i is gettered (dissolved) by the iron film, and part — diffuses into the crystal volume. The possibility of the process of zinc atoms being gettered by metal films was reported in [14,15]. During the annealing process, the zinc from the surface of the iron film evaporates and enters the „free“ surface through the atmosphere in which the doping takes place. The gettering of Zn_i in the studied crystals takes place both on the doping surface and, most likely, on the surfaces of „chipping“. Zinc atoms, having got on „free“ surface of the crystal, begin to diffuse into its volume and form complexes with other point defects and impurities. A similar process occurs during annealing and doping of ZnSe crystals in a zinc atmosphere. This explains why the characteristics of the „free“ surface after doping in argon are close to those of crystals annealed in a zinc atmosphere and doped with iron in a zinc atmosphere. This hypothesis also explains that the width of the area *3* increases with increasing doping time.

From the proposed hypothesis, it follows that the lines 628 and 541 nm are formed by complexes that include intergranular zinc. In the literature [16] a line with characteristics (maximum, spectral width) similar to the 628 nm line is associated with the luminescence of the donor-acceptor pair $\{O_{Se} \cdot Zn_i^{\bullet} V_{Zn}//\} - Zn_i^{\bullet}$. This line is observed in the area *3* in its separate regions.

A similar (maximum, spectral width) to the 541 nm line has been observed [15,16] in copper-doped crystals. This

line is thought to be formed by the luminescence of a donor-acceptor pair, which includes copper (more likely as an $Cu_{Zn}-Cu_i$) center) and as a minor donor — its own defect. According to our ideas, this small donor is, as in the case of the 628 nm line, Zn_i.

As can be seen from the table, the studied crystals contain copper, so the formation of such a complex is possible. Given this hypothesis and taking into account that the spectrum of the area *3* includes the line 541 nm forming ELIA, it is the interstitial zinc becomes the point defect, which, according to the data of [10], is formed in the doping area during the doping of ZnSe crystals with iron. As noted above, it is assumed that part of the Zn_i formed during the doping process diffuses into the crystal volume and forms complexes with other defects. The spatial distribution of these complexes will correlate with the spatial distribution of interstitial zinc. The luminescence of these complexes will lead to the ELIA formation. This explains that both in the ELIA and in the area *3* the luminescence of the 541 nm line dominates, since the nature of the — complex Zn_i with some background impurity — is the same.

The 570 nm line dominating in the spectrum of the area *4* by its characteristics (position of the maximum, line width) is close to the IDC luminescence, which in [17] is associated with excess selenium.

Thus, as a result of the standard procedure of iron doping of ZnSe crystals, regions adjacent to all its surfaces are formed in them, the luminescence characteristics and composition of the IDC of which differ significantly from those of these samples' volumes. The doped sample appears to be surrounded by these regions from all its surfaces. The depth of penetration of these areas into the sample volume depends on the doping time and can be of the order of several hundred microns. This must be taken into account when using for research methods in which the excitation of carriers occurs in a narrow (several μm thick) near-surface layer. It is clear that the influence of doping on the surface of the chip due to their contamination with iron during the sputtering of the iron film can be avoided. But then the chipping surfaces become similar to the free surface and areas {*3* are formed on them. To prevent the formation of these areas during doping in an inert gas atmosphere, it is probably possible only by covering all crystal surfaces with some material. However, in this case, other problems may arise, such as contamination of the near-surface regions with this material. Most likely, the situation with the formation of large-scale near-surface regions with properties different from the main volume in crystals that have undergone the procedure of doping by means of HTD, is quite general (at least for multicomponent semiconductors).

5. Conclusion

1. Doping of ZnSe with iron from a metal film using HTD in an argon atmosphere leads to the formation of areas with altered properties on all surfaces of the doped sample, the sizes of which increase with increasing doping time and can reach $500-1000\,\mu$m.

2. These areas are formed, among other things, as a result of gettering by the iron film of zinc atoms and their subsequent evaporation and transfer through the doping atmosphere to „free" surfaces of the crystal.

3. It is shown that the point defect, the formation of which leads to the formation of ELIA in this method of doping is likely to be Zn_i, and the ELIA itself is the result of luminescence of the donor-acceptor pair $Cu-Zn_i$.

4. The obtained results indicate that the possibility of forming large-scale areas with different characteristics from the volume during doping of the crystal from all its sides should be taken into account. This is especially necessary when using the so-called surface and integral methods of investigation.

Funding

The research was supported by the Russian Science Foundation (grant No. 23-23-00512, https://rscf.ru/project/23-23-00512/) concerning the development of the method and creation of samples Fe^{2+}: ZnSe.

Conflict of interest

The authors declare that they have no conflict of interest.

References

[1] S. Fusil, P. Lemasson, J.-O. Ndap, A. Riviére, G. Neu, E. Tournı̄, G. Geoffroy, A. Zozime, R. Triboulet. J. Cryst. Growth, **184**–**185**, 102 (1998).
[2] S.A. Rodin, V.B. Ikonnikov, D.V. Savin, E.M. Gavrishchuk. Neorg. mater, **53** (11), 1143 (2017). (in Russian).
[3] V.P. Kalinushkin, O.V. Uvarov. ZhTF, **86** (12), 119 (2016). (in Russian).
[4] V.P. Kalinushkin, O.V. Uvarov, A.A. Gladilin. J. Electron. Mater., **47**, 5087 (2018).
[5] G. Steinmeyer, J.W. Tomm, P. Fuertjes, U. Griebner, S.S. Balabanov, T. Elsaesser. Phys. Rev. Appl., **19**, 054043 (2023).
[6] D.V. Martyshkin, V.V. Fedorov, M. Mirov, I. Moskalev, S. Vasilyev, S.B. Mirov. *CLEO: Science and Innovations 2015* (San Jose, California, US, 2015). https://doi.org/10.1364/CLEO_SI.2015.SF1F.2
[7] S.D. Velikanov, N.A. Zaretsky, E.A. Zotov, S.Y. Kazantsev, I.G. Kononov, Y.V. Korostelin, A.A. Maneshkin, K.N. Firsov, M.P. Frolov, I.M. Yutkin. Kvant. elektron., **46** (1), 11 (2016). (in Russian).
[8] K.N. Firsov, E.M. Gavrishchuk, S.Yu. Kazantse, I.G. Kononov, S.A. Rodin. Laser Phys. Lett., **11**, 085001 (2014). DOI: 10.1088/1612-2011/11/8/085001.
[9] K. Karki, S. Yu, V. Fedorov, Y. Wu, S. Mirov. In: *Laser Congress 2020 (ASSL, LAC),* P. Schunemann, C. Saraceno, S. Mirov, S. Taccheo, J. Nilsson, A. Petersen, D. Mordaunt, J. Trbola (eds) [OSA Technical Digest (Optica Publishing Group, 2020) p. AW1A.3].

[10] V. Kalinushkin, O. Uvarov, S. Mironov, K. Nartov, N. Il'ichev, M. Studenikin, E. Gavrischuk, N. Timofeeva, S. Rodin, A. Gladilin. J. Luminesc., **231**, 117795 (2021). https://doi.org/10.1016/j.jlumin.2020.117795
[11] T.V. Kotereva, V.B. Ikonnikov, E.M. Gavrishchuk, A.M. Potapov, D.V. Savin. ZhTF **7**, 1110 (2018). (in Russian).
[12] D.D. Nedeoglo, A.V. Simashkevich. *Electricheskie i luminescentnye svoistva selenids zinka* (Kishinev, Shtiyintza, 1984) p. 53. (in Russian).
[13] Li Huan-Yong, Jie Wan-Qi, Zhang Shi-An, Sun Zhen-Rong, Xu Ke Wei. Chin. Phys. Soc., **15** (10), 2407 (2006).
[14] A.N. Georgobiani, M.K. Sheynkman. *Fizika soyedineniy* $A^{II}B^{VI}$ (M., Nauka, 1986) p. 72. (in Russian).
[15] G.N. Ivanova, V.A. Kasyan, D.D. Nedeoglo, S.V. Oprya. FTP, **32** (2), 171 (1988). (in Russian).
[16] N.K. Morozova, E.M. Gavrishchuk, I.A. Karetnikov, O.R. Golovanova, V.S. Zimogorskii, V.G. Galstyan. Zhurn. prikl. spektroskopii **5**, 731 (1996). (in Russian).
[17] I. Avetissov, K. Chang, N. Zhavoronkov, A. Davydov, E. Mozhevitina, A. Khomyakov, S. Kobeleva, S. Neustroev. J. Cryst. Growth, **401**, 686 (2014). DOI: 10.1016/j.jcrysgro.2014.01.003

Translated by J.Savelyeva